Yuzuncu Yil University
Journal of the Institute of Natural & Applied Sciences

Research Article

# Synthesis and Characterization of Stannic Oxide (SnO₂) Thin Film

## Reşit ÖZMENTEŞ

Bitlis Eren University, Vocational School of Health Services, 13100, Bitlis, Türkiye
Reşit ÖZMENTEŞ, ORCID No:0000-0002-5893-0660
Corresponding author e-mail: rozmentes@beu.edu.tr

**Abstract:** $SnO_2$ (Stannic oxide) thin films were prepared by atomizing stannic chloride ($SnCl_4$) solution onto microscope slide substrate at 400°C substrate temperature with a simple spray coating device. The samples were examined optically, structurally, morphologically, and compositionally by UV-Vis, XRD, SEM and EDS spectroscopic techniques. Optical analysis showed that the synthesized films had 70–88% transmittance in the visible region and the band gap energy ($E_g$) value was 3.89 eV. Based on absorbance and transmittance measurements, the wavelength-dependent refractive index distribution of the film was found and its thickness was calculated as 239 nm by the Swanepoel method. XRD studies determined that the films are amorphous structure. FE-SEM micrographs revealed that granular structure with a size of 884 nm, and a film thickness around 287.1-341.8 nm while the EDX analysis indicated the non-stoichiometric structure of the deposited thin films.

## Stannik Oksit (SnO₂) İnce Film Sentezi ve Karakterizasyonu

**Öz:** $SnO_2$ (stannik oksit) ince filmler, stannik klorür ($SnCl_4$) çözeltisinin basit bir sprey kaplama cihazı ile 400°C altlık sıcaklığında mikroskop lam altlığı üzerine atomize edilmesiyle hazırlandı. Numuneler UV-Vis, XRD, SEM ve EDS spektroskopik teknikleri ile optiksel, yapısal, morfolojik ve bileşimsel olarak incelenmiştir. Optik analiz, sentezlenen filmlerin görünür bölgede %70-88 geçirgenliğe sahip olduğunu ve bant aralığı enerji ($E_g$) değerinin 3.89 eV olduğunu gösterdi. Absorbans ve geçirgenlik ölçümlerine dayalı olarak filmin dalga boyuna bağlı kırılma indisi dağılımı bulunmuş ve Swanepoel yöntemi ile kalınlığı 239 nm olarak hesaplanmıştır. XRD çalışmaları filmlerin amorf yapıda olduğunu belirlemiştir. FE-SEM mikrografları, 884 nm boyutunda granüler yapıyı ve 287.1-341.8 nm civarında film kalınlığını ortaya koyarken, EDX analizi, biriktirilen ince filmlerin stokiyometrik olmayan yapısını gösterdi.

## 1. Introduction

Functional materials known as metal oxides can display various properties, including being an insulator, semiconductors, metals or superconductors. Tin oxides-$SnO_x$ (stannous-SnO, stannic-$SnO_2$) are metal oxides with a wide semiconductor band gap from the class of transparent conductive oxide (TCO) material owing to showing excellent electrical conductivity and transmittance in the visible region of light (Nikiforov et al., 2020). The basic requirement for TCO film is low resistivity (<0.001 Ω.cm), wide bandgap (>3.5 eV) and high optical transmittance (>90%) (Timofeev et al., 2020).

Among many TCOs, tin oxide films have received the most research attention due to their high transmittance, high carrier concentration ($10^{19}$-$10^{21}$cm$^{-3}$), wide bandgap, high electrical as well as thermal conductivity (Gong et al., 2019; Dalapati et al., 2021). Due to the variable oxidation states and oxygen vacancy defects, tin oxides have versatile applications in various fields (Anu & Savitha Pillai, 2022). Tin oxides are widely used as semiconductor materials in diodes, transistors, solar cells, LEDs, gas sensors, capacitors, photocatalytic, optoelectronic devices, and many other electronic devices (Schell et al., 2017; Doyan et al., 2021).

SnO$_x$ has two main oxide phases: stannic-SnO$_2$ and stannous-SnO. In these phases tin has the oxidation state of Sn$^{4+}$ and Sn$^{2+}$, respectively (Dias et al., 2020). The SnO and Sn$_2$O$_3$-Sn$_3$O$_4$ oxidation phases of tin oxide are more difficult to synthesize because they indicate thermal instability at temperatures above 400 ºC (Suman et al., 2015).

Stannous oxide (SnO) generally shows p-type semiconductor properties with a wide band gap (2.5-3.4 eV) and crystallizes in an orthorhombic crystal structure. Stannic oxide (SnO$_2$) is an n-type semiconductor with a broad bandgap (3.6-4 eV) and crystallizes in the tetragonal rutile structure (with the values of lattice parameters a=b=0.4738, c=0.3187 nm and space group P42/mnm) (Abdullah et al., 2018). When exposed to extreme pressure and temperatures, tin can adopt a metastable orthorhombic crystal structure. This structure involves each tin atom bonding with six oxygen atoms, while each oxygen atom, in turn, bonds with the three nearest tin atoms to form an equilateral triangle (Patil et al., 2012).
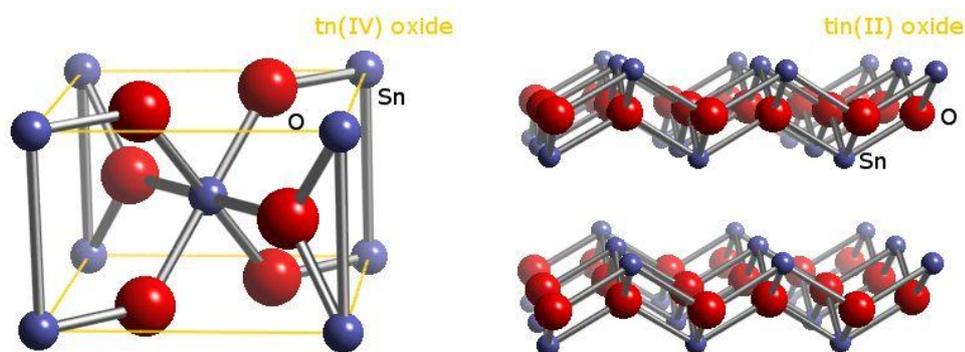


Figure 1. The crystal structure of tin oxides (Hafez, 2014).

Microstructural and optoelectronic properties of tin oxide are strongly dependent on the fabrication circumstance and technique. Various techniques are usedfor depositing tin oxide films, such asthermal evaporation, electrodeposition, chemical vapor deposition, and sol-gel spray. The spraying method is an important technique that is used for the synthesis of tin(II) oxideonto a hot substrate at high temperatures (400-600ºC) (Dalapati et al., 2021). It is an essential alternative to other methods for its easy feasibility, homogeneous distribution, and economic efficiency (low cost-effectiveness). At the same time the method is one of the low-cost and simple methods used to coat large areas of SnO$_2$ films at low coating temperatures (Al-Jawad et al., 2015). The quality of the sprayed films is directly affected by the type of precursor and deposition temperature. Palanichamy et al. (2018) reported that SnO$_2$ thin films produced by the nebulizer spray pyrolysis method at different deposition temperatures (300-500 C) have a tetragonal crystal structure. Thanachayanont et al. (2011) produced SnO$_2$ films at 300, 400 and 500 ºC by spray pyrolysis method on soda-lime glass substrate from SnCl$_2$solution containing 90% methanol, 10% deionized water and SnCl$_2$ precursor. According to the study, films produced at 300 C had an amorphous structure consisting of small circular surface grains, while films produced at 400 and 500 C showed a polycrystalline structure with larger grains. In another study, Caglar et al. (2007) synthesized amorphous SnO$_2$ thin films from SnCl$_4$.5H$_2$O precursor on glass substrate by spray pyrolysis method at 300 C substrate temperature. Similarly, Pan & Fu (2001) reported that tin oxide films deposited at substrate temperature below 300 °C form an amorphous structure. Generally, in the synthesis of sol-gel based SnO$_2$ thin films, the starting solution had been prepared by dissolving powder SnCl$_2$ or SnCl$_4$ in suitable solvents. Therefore, the current

study aims to produce tin oxide thin films from liquid SnCl₄ precursor by spray method and to examine their optical, structural, morphological and compositional properties.

## 2. Material and Methods

### 2.1. Material

In this study, stannic chloride ($SnCl_4$) anhydrous (98%) inorganic compound was used as the precursor. $SnCl_4$ is a colorless, hygroscopic (water-sensitive), fuming liquid that dissolves in cold water and decomposes in hot water to form hydrochloric acid (HCl). It fumes when it comes into contact with air. Methanol (98%), ethanol (90%), deionized water was used as solvents and diluted HCl (%30) solution was used as stabilizer.

### 2.2. Sample preparation

The spraying solution was prepared at room temperature with liquid tin(IV) chloride as a precursor, deionized water and methanol as a solvent. For this, a solution was prepared using 3 ml of tin(IV) chloride, 5 ml of deionized water, 90 ml of methanol and 2 ml of HCl. After stirring the mixture for an hour at room temperature on a magnetic stirrer, 100 ml tin chloride precursor solution was obtained. The glass substrates were chemically cleaned with ethanol and distilled water, placed on a flat surface heater, and the heater brought to the desired temperature of 400 °C. Then, the starting solution was sprayed from a distance of 30 cm on a glass slide target. A simple air compressor and nebulizer were used for the spraying process. The thin film coating process was completed by the evaporation of the solution reaching the substrate surface by spraying the precursor solution with the help of a nebulizer with constant pressure air.

The possible chemical reaction occuring on the heated substrate is as follows (Bari & Patil, 2014; Al-Jawad et al., 2015):

$$SnCl_4.5H_2O \rightarrow SnO_2 + 3H_2O + 4HCl \tag{1}$$

The quality of thin films strongly depends on the coating conditions and the setting of their parameters. During the experiment, the distance between the substrate-spray nozzle was maintained at 30 cm, the solution flow rate was approximately 5 ml/min, and the deposition temperature was kept at 400 °C.

## 3. Results and Discussion

### 3.1. Optical properties

Optical analysis were carried out by taking absorbance and transmittance measurements of the samples in the 300-900 nm wavelength range with a Shimadzu-2450 UV-Vis spectrophotometer. The optical band gap energy ($E_g$) of the films was found by plotting the absorption coefficient ($\alpha$) versus wavelength. The $E_g$ value was calculated using Equation (2) with the well-known Tauc method (Marikkannan et al., 2015). Accordingly, the absorption coefficient ($\alpha$) and the incident photon energy (hν) depend as follows (Thirumoorthi & Prakash, 2016).

$$\alpha h\nu = A(h\nu - E_g)^n \tag{2}$$

here, A is a constant, and n depends on the optical transition type (n=1/2 for direct and n=2 for indirect transition).

If both sides of the equation are squared (A=1 and n=1/2), the absorption coefficient $\alpha$ can also be expressed as:

$$(\alpha h\nu)^2 = h\nu - E_g \qquad (3)$$

In the graph of $(\alpha h\nu)^2$ vs. $h\nu$, the band gap value is found from the point where it intersects the x-axis by extrapolating the linear part of the curve. UV-vis spectral investigations were carried out to investigate the optical properties of tin oxide films. Optical absorption and transmission spectra in the wavelength range of 300 to 400 nm were recorded to calculate the bandgap of the film. The $(\alpha h\nu)$-$(h\nu)$ graph was drawn to find the optical forbidden energy gap value of the film. In this graph, the forbidden band gap ($E_g$) of the film is found from the photon energy value corresponding to the wavelength where the absorption sharply increases. The absorption spectrum of the tin oxide thin film sprayed on the glass substrate is shown in Figure 2a. It is understood that high photon absorption occurs in the UV region of the spectrum around the 320 nm wavelength (band edge). This is the point corresponding to the band gap energy of the thin film. The optical transmittance spectrum of tin oxide thin film is shown in Figure 2b. From the graph; it is evident that the film has a high level of transparency (max 88%) in the visible and near-infrared region at wavelengths above 400 nm. The transmittance spectrum is in the form of interference fringes (presence of oscillations) in the range of 350-800 nm, indicating that the films are formed homogeneously.



(a)                                         (b)
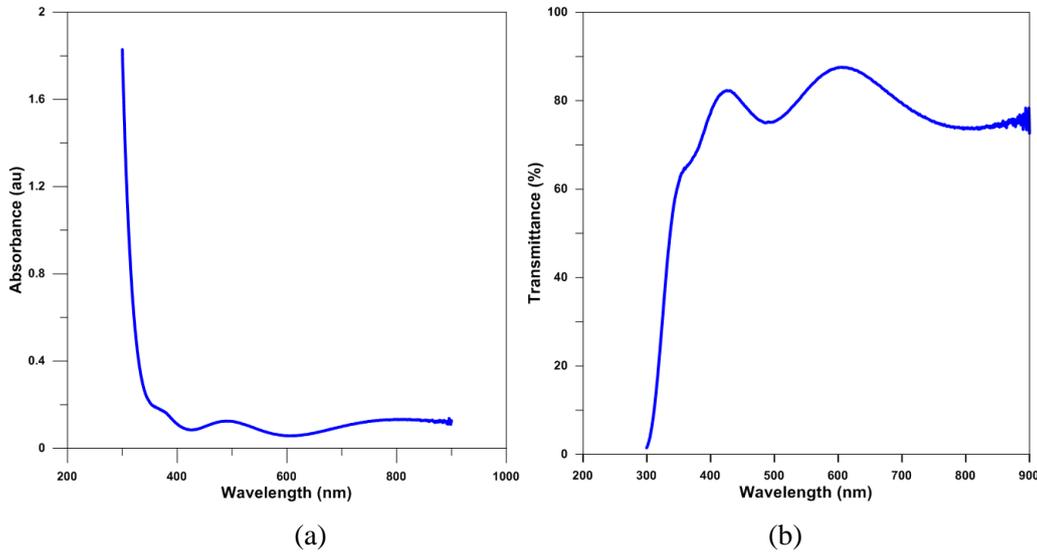
Figure 2. Variation of (a) absorbance (b) transmittance spectra as function of wavelength for tin oxide thin film.

The thickness of the film can be calculated from the successive max or min wavelengths in the transmittance spectrum by the Swanepoel method using Equation (4) (Akgul et al., 2013)

$$d = \frac{\lambda_1 \lambda_2}{2(n_1\lambda_2 - n_2\lambda_1)} \qquad (4)$$

where, d is thickness, $n_1$ and $n_2$ are the values of refractive indices calculated at wavelengths $\lambda_1$ and $\lambda_2$. Figure 3a shows that the consecutive maximum points correspond to wavelengths of approximately 430 and 600 nm. The wavelength-dependent refractive index distribution of the film was obtained as in Figure 3b based on optical absorbance and transmittance measurements. From here, the $n_1$ and $n_2$ values corresponding to the $\lambda_1$ and $\lambda_2$ wavelengths were found to be 2.709 and 2.527, respectively. As a result of all calculations, the thickness of the film was found to be 239 nm using Equation (4). This value is a reasonable nanofilm thickness. In their similar study, Orimi & Maghouili (2016) have been calculated the thickness of the SnO2 nanostructured film using the Swanepole method. To find the thickness, the authors calculated the $n_1$ and $n_2$ refractive index values, corresponding to the two consecutive maximum or minimum transmittance values in formula (4), by taking them as approximately 2 and estimated them as 422 nm. However, in this study, $n_1$ and $n_2$

values were calculated directly from the refractive index distribution obtained from absorption and transmittance measurements. In this respect, the thickness value of the film calculated in this study is highly reasonable. The $E_g$ value was calculated as 3.89 eV, as shown in Figure 3b. This value is close to the pure $SnO_2$ band gap of 3.6 eV. The slight increment in the band gap value is interpreted to be due to the deviation in the stoichiometry of the point defect concentration associated with the crystal structure of the $SnO_2$ films (Khaenamkaew et al., 2020). It should be noted that, the optical band gap value calculated in this study is in agreement with the band gap values in the literature value (3.6-4 eV) for stannic oxide thin films (Erken & Gümüş, 2018; Gong et al., 2019).
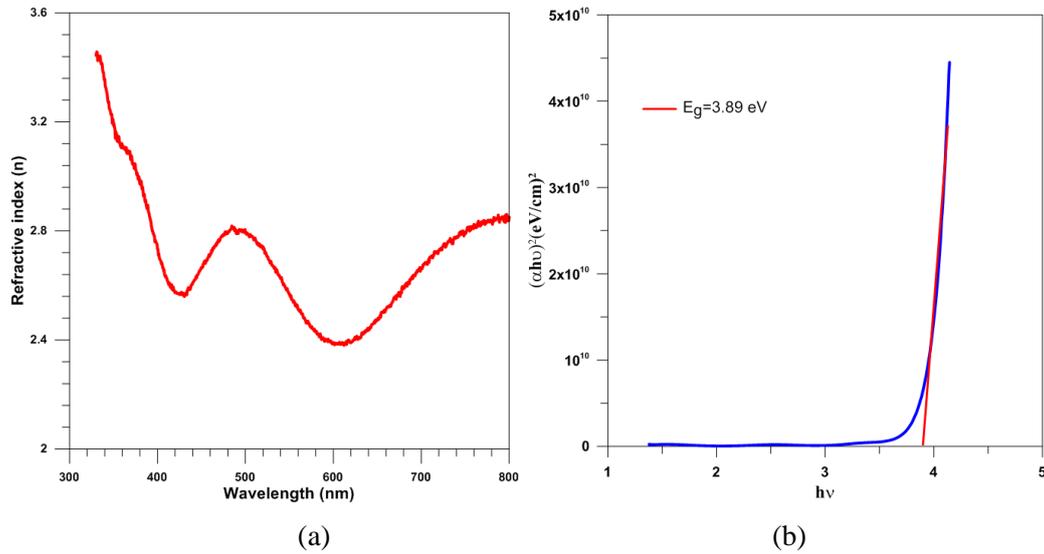


Figure 3. (a) Wavelength-dependent refractive index dispersion of the film. (b) The $(\alpha h\nu)^2$ vs $(h\nu)$ plot of tin oxide thin film.

## 3.2. XRD results

The crystal and phase structure of tin oxide thin films were investigated by X-ray diffraction method. Figure 4 shows the XRD pattern in the angle range $2\theta=0°-80°$. The presence of large mound in the XRD pattern in the angle range from 10° to 40° and the absence of sharp diffraction peaks confirm the amorphous nature of the film. Low-intensity peaks appearing in the spectrum, such as the two peaks centered at $2\theta=23°$ and $27.7°$ at the top of the large bump, can be considered an indication that the film is close to transformation from the amorphous phase to polycrystalline phase. The absence of characteristic peaks in the spectrum is associated with the inability of tin to crystallize by combining with oxygen due to the stoichiometric deviation, impurities merger in synthesis process and some structural defects (Gomaa et al., 2022; Nwanna et al., 2022). The fact that the tin oxide film does not form in a crystal structure can be attributed to the reasons arising from the insufficient thickness of the film. In the current study, the 239 nm thickness of the tin oxide film has not been sufficient for the grains to accumulate and crystallize into a nanostructured thin film layer. Literature studies show that tin dioxide and other optical materials are formed in the crystalline phase when the film thickness is around 400 nm or greater, which is greater than the thickness of our sample (Lee et al., 2014; El-Denglawey et al., 2018). Another point that should not be overlooked is that in most cases the thin oxide films are subjected to thermal annealing to ensure crystallization of the film in tetragonal and other phases (Mehraj et al., 2015; Sarıtaş, 2023).
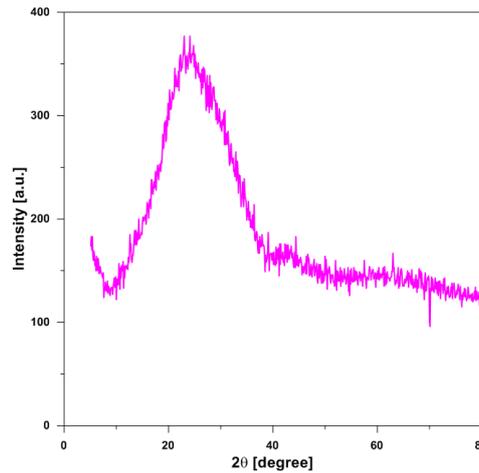
Figure 4. XRD patterns of the tin oxide films.

## 3.3. Morphological and compositional analysis

The morphological characteristics of tin oxide thin film were analyzed by Field Emission Scanning Electron Microscope (FE-SEM). The detailed FE-SEM images of the samplesin Figure 5-(a)-(d) magnified 20 Kx (20000 times magnification), 50 Kx and 200 Kx, it is seen that the closely arranged spherical grains of tin oxide are agglomerated on the film surface. The average radius of the spheric granular regions was measured as 884 nm, as illustrated in Figure 5-(c). In the images, although the sizes of the particles in the granular regions of the film layer vary, homogeneity is observed. There are nanoscale boundaries between particles. It can be seen from Figure 5-c that the average grain size of the smallest particle is around 20 nm. This means that since the tin was not fully oxidized on the substrate temperature at 400$^{\circ}$C, the particles could not grow fully and a dense particle accumulation did not occur. Therefore, the crystal phase did not fully emerge as seen in XRD spectroscopy. As seen in the cross-sectional image in Figure 5-d, the surface of the tin oxide film coated on the glass substrate is rough. There is an average thickness due to the rough surface of the film. From the cross-sectional FE-SEM micrograph, the film thickness was measured as 287.1 and 341.8 nm in near two region. These thickness values are consistent with the 239 nm value calculated from optical spectroscopic measurements. The fluctuation in the film thickness value is closely related to the dispersion format of microparticles during the atomization and deposition of the $SnCl_4$ starting solution during production.

Tin oxide sample was analyzed for elemental composition using EDX system connected to SEM setup. The elemental analysis was performed for Sn and O. The average atomic percentage was 21.22: 36.71. The % of Sn and O should be stoichiometrically at 33.30 and 66.70, respectively (Bari & Patil, 2014). The average results are presented in Table 1. There is quite a deviation from the stoichiometry of the film. Figure 6 shows the EDX spectrum of tin oxide thin film. The spectrum presents well-defined peaks of tin and oxygen, revealing the presence of silicon detected from the substrate. Si, C, Ca and Cu, which emerged in the EDX analysis of the material, are the elements found in the structure of the glass substrate.

Table 1. The average atomic percentage of the tin oxide sample

| Element | Weight (%) | Atomic (%) |
|---|---|---|
| Tin(Sn) | 58.45 | 21.22 |
| Oxygen(O) | 13.63 | 36.71 |
| Chorine(Cl) | 0.77 | 0.94 |
| Carbon(C) | 3.91 | 14.04 |
| Silicon(Si) | 12.04 | 18.46 |
| Calcium (Ca) | 2.62 | 2.81 |
| Copper (Cu) | 8.58 | 5.82 |
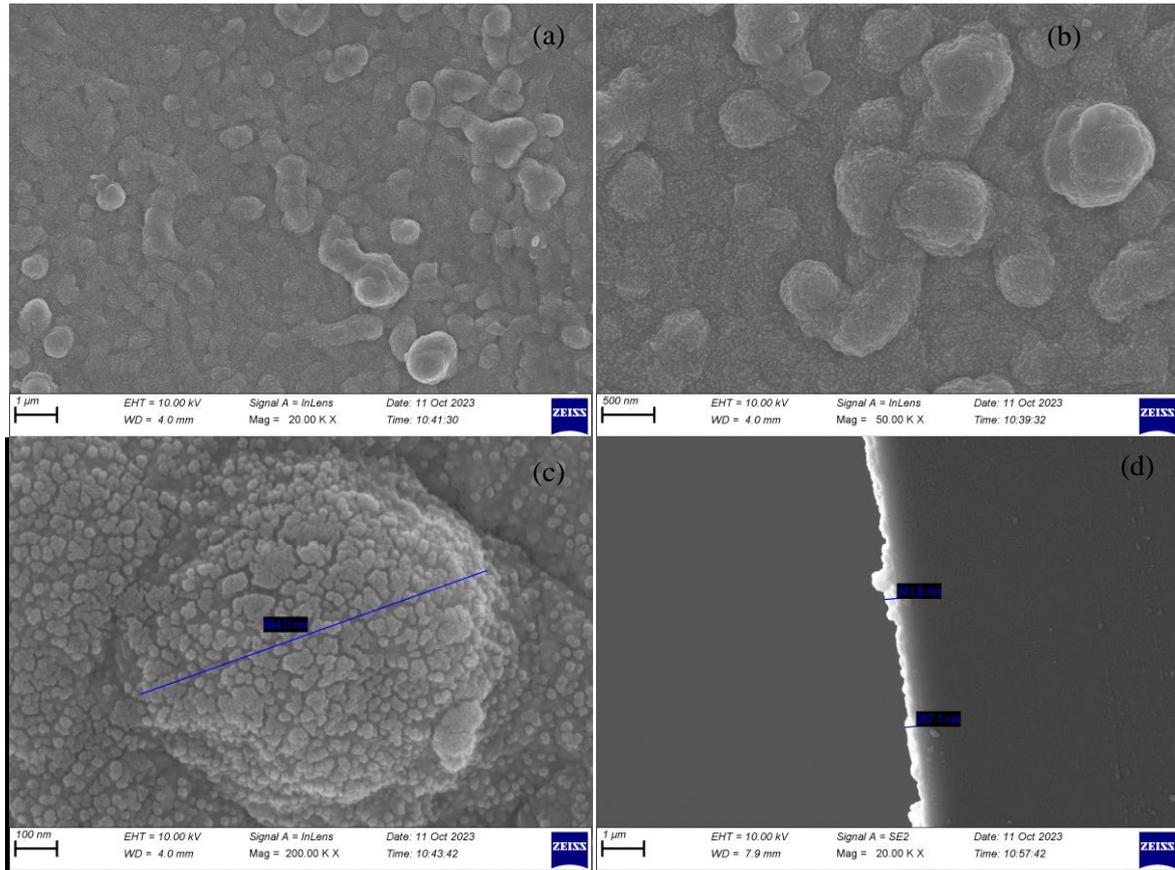
Figure 5. FE-SEM images of the tin oxide thin film at different magnifications. (a) magnification at 1μm scale (b) magnification at 500 nm scale (c) average grain size of tin oxide nanoparticless (d) cross sectional image of tin oxide film on glass substrate.
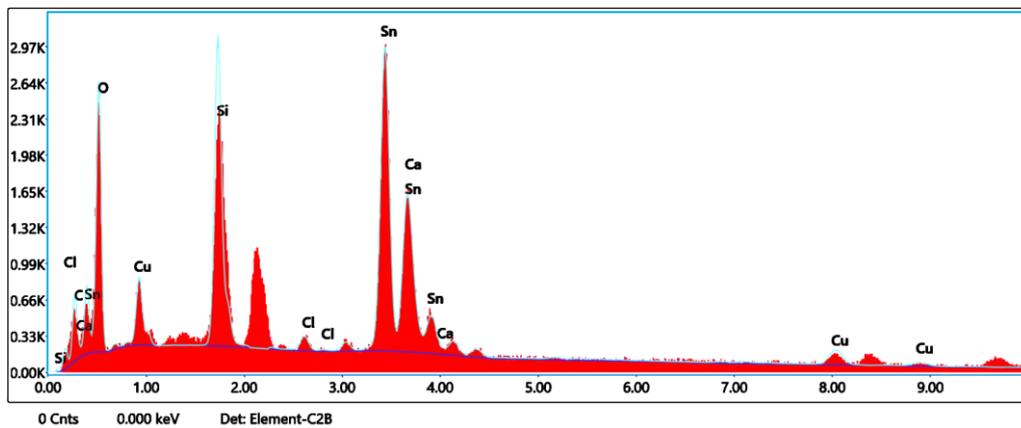


Figure 6. EDX spectra of the tin oxide film.

## 4. Conclusion

Tin oxide thin films were produced using $SnCl_4$ precursor on microscope slide at 400 °C substrate temperature by sol-gel spray deposition method. Absorption coefficient, band gap (3.89 eV) and refractive index distribution were derived from optical absorption and transmittance measurements. The thickness of the film was calculated as 239 nm using the Swanepoel method from the interference fringes observed in the transmittance spectrum. The XRD results showed that the deposited tin oxide films were amorphous nature. The non-crystalline structure of the film was ascribed to stoichiometric deviation due to impurities merger in synthesis process and some structural

defects. FE-SEM micrographs indicated the granular structure of the film surface and the film thickness was around 287.1-341.8 nm. EDX spectra revealed non-stoichiometric composition with the presence of 22.4% tin (Sn) and 36.71% oxygen (O) elements in the film. These results demonstrate that the amorphous tin oxide thin films produced 400 °C substrat temperature can be used for a variety of semiconductor transparent conductive oxide (TCO) applications.

## References

Abdullah N., Ismail N. M., & Nuruzzaman D. M. (2018). Preparation of tin oxide ($SnO_2$) thin films using thermal oxidation. *IOP Conference. Series: Material Science Engineering*, 319, 012022. doi:10.1088/1757-899X/319/1/012022

Akgul, F. A., Gumus, C., Er, A. O., Farha, A. H., Akgul, G., Ufuktepe, Y., & Liu, Z. (2013). Structural and electronic properties of $SnO_2$. *Journal of Alloys and Compounds*, 579, 50-56. doi:10.1016/j.jallcom.2013.05.057

Al-Jawad S. M. H., Oleiwe F. H., & Khulaef, J. H. (2015). Preparation and characterization of Tin Oxide thin films by using spray pyrolysis technique. *Engineering & Technical Journal*, 33(B), 3. doi:10.30684/etj.33.3B.12

Anu, M. A., & Savitha Pillai, S. (2022). Structure, thermal, optical and dielectric properties of $SnO_2$ nanoparticles-filled HDPE polymer. *Solid State Communications*, 341, 114577. doi:10.1016/j.ssc.2021.114577

Bari, R. H., & Patil, S. B. (2014). Studies on spray pyrolised nanostructured $SnO_2$ thin films for $H_2$ gas sensing application. *International Letters of Chemistry, Physics and Astronomy*, 17(2), 125-141. doi:10.56431/p-5f086q

Caglar, Y., Ilican, S., & Caglar, M. (2007). Single-oscillator model and determination of optical constants of spray pyrolyzed amorphous $SnO_2$ thin films. *The European Physical Journal B*, 58, 251-256. doi:10.1140/epjb/e2007-00227-y

Dalapati, G. K., Sharma, H., Guchhait, A., Chakrabarty, N., Bamola, P., Liu, Q., ..., & Sharma, M. (2021). Tin oxide for optoelectronic, photovoltaic and energy storage devices: A review. *Journal Material Chemistry A*, 9, 16621. doi:10.1039/d1ta01291f

Dias, J. S., Batista, F. R. M., Bacani R., & Triboni, E. R. (2020). Structural characterization of SnO nanoparticles synthesized by the hydrothermal and microwave routes. *Scientific Reports/Nature Research*, 10, 9446. doi:10.1038/s41598-020-66043-4

Doyan, A., Susilawati, Muliyadi, L., Hakim, S., Munanadar, H., & Taufik, M. (2021). The effect of dopant material to optical properties: energy band gap Tin Oxide thin film. *Journal of Physics: Conference Series*, 1816, 012114. doi:10.1088/1742-6596/1816/1/012114

El-Denglawey, A., Makhlouf, M. M., & Dongol, M. (2018). The effect of thickness on the structural and optical properties of nano Ge-Te-Cu films. *Results in Physics*, 10, 714-720. doi:10.1016/j.rinp.2018.07.023

Erken, Ö., & Gümüş, C. (2018). Determination of the thickness and optical constants of polycrystalline $SnO_2$ thin film by envelope method. *Adıyaman University Journal of Science*, 8(2), 141-145.

Gomaa, H. M., Yahia, I. S., Yousef, E. S., Zahren, H. Y., Makram, B. M. A., & Saudi, H. A. (2022). A novel correction method toward extraction of reflectance and linear refractive index of some borosilicate glasses doped with $BaTiO_3$. *Journal of Electronic Materials*, 51, 6347-6355. doi:10.1007/s11664-022-09858-3

Gong, J., Wnag, X., Fan, X., Dai, R., Wang, Z., Zhang, Z., & Ding, A. Z. (2019). Temperature dependent optical properties of $SnO_2$ film study by ellipsometry. *Optical Materials Express*, 9(9), 3691-3699. doi:10.1364/OME.9.003691

Hafez, A. (2014). *Development of enhanced hydrogen-doped indium oxide material properties by integration of a negatively biased mesh into the sputtering process.* (MSc), Technical University of Berlin, Berlin Institute of Technology, Berlin, Germany.

Khaenamkaew, P., Manop, D., Tanghengjaroen, C., & Ayuthaya, W. P. N. (2020). Crystal structure, lattice strain, morphology, and electrical properties of $SnO_2$ nanoparticles induced by low calcination temperature. *Advance in Materials Science and Engineering*, 10, Article ID 3852421. doi:10.1155/2020/3852421

Lee, S. M., Joo, Y. H., & Kim, C. I. (2014). Influences of film thickness and annealing temperature on propertiesof sol–gel derived ZnO–SnO$_2$ nanocomposite thin film. *Applied Surface Science*, 320, 494-501. doi:10.1016/j.apsusc.2014.09.099

Marikkannan, M., Vishnukanthan, V., Vijayshankar, A., Mayandi J., & Pearce, J. M. (2015). A novel synthesis of tin oxide thin films by the sol-gel process for optoelectronic applications. *AIP* Advances, 5, 027122. doi:10.1063/1.4909542

Mehraj, S., Ansari, M. S., & Alimuddin. (2015). Annealed SnO$_2$ thin films: Structural, electrical and their magnetic properties. *Thin Solid Films*, 589, 57-65. doi:10.1016/j.tsf.2015.04.065

Nikiforov, A., Timofeev, V., Mashanov, V., Azarov, I., Loshkarev, I., Volodin, V., Gulyaev, D., Chetyrin, I., & Korolkov, I. (2020). Formation of SnO and SnO$_2$ phases during the annealing of SnO(x) films obtained by molecular beam epitaxy. *Applied Surface Science*, 512, 145735. doi:10.1016/j.apsusc.2020.145735

Nwanna, E. C., Imoisili, P. E., & Jen, T. C. (2022). Synthesis and characterization of SnO$_2$ thin films using metalorganic precursors. *Journal of King Saud University-Science*, 34, 102123. doi:10.1016/j.jksus.2022.102123

Orimi, R. L., & Maghouli, M. (2016). Optical characterization of SnO$_2$ nanostructure thin films, annealed at different temperatures. *Optik*, 127, 263-266. doi:10.1016/j.ijleo.2015.10.033

Palanichamy, S., Mohamed, J. R., Kumar, P. S. S., Pandiarajan, S., & Amalraj, L. (2018). Physical properties of nebulized spray pyrolysised SnO$_2$ thin films at different substrate temperature. *Applied Physics A*, 124, 643. doi:10.1007/s00339-018-2065-8

Pan, X. Q., & Fu, L. (2001). Oxidation and phase transitions of epitaxial tin oxide thin films on sapphire. *Journal of Applied Physics*, 89, 6048-6055. doi:10.1063/1.1368865

Patil, G. E., Kajale, D. D., Gaikwad, V. B., & Jain, G. H. (2012). Spray pyrolysis deposition of nanostructured tin oxide thin films. *International Scholarly Research Network ISRN Nanotechnology*, 5. doi:10.5402/2012/275872

Sarıtaş, S. (2023). The effect of annealing temperature on iron-doped tungsten oxide structure and photosensitive gas sensor applications. *Erzincan University Journal of Science and Technology*, 16(2), 374-383. doi:10.18185/erzifbed.1277351

Schell, J., Lupascu, D. C., Carbonari, A. W., Mansano, R. D., Dang, T. T., & Vianden, R. (2017). Implantation of cobalt in SnO$_2$ thin films studied by TDPAC. *AIP Advances*, 7, 055304. doi:10.1063/1.4983270

Suman, P. H., Felix, A. A., Tuller, H. L., Varela, J. A., & Orlandi, M. O. (2015). Comparative gas sensor response of SnO$_2$, SnO and Sn$_3$O$_4$ nanobelts to NO$_2$ and potential interferents. *Sensors and Actuators B*, 208, 122-127. doi:10.1016/j.snb.2014.10.119

Thanachayanont, C., Yordsri, V., & Boothroyd, C. (2011). Microstructural investigation and SnO nanodefects in spray-pyrolyzed SnO$_2$thin films. *Materials Letters*, 65, 2610-2613. doi:10.1016/j.matlet.2011.05.071

Timofeev, V. A., Mashanov, V. I., Nikiforov, A. I., Azarov, I. A., Loshkarev, I. D. Korolkov, I. V., Gavrilova, T. A., Yesin, M. Y., & Chetyrin, I. A. (2020). Effect of annealing temperature on the morphology, structure, and optical properties of nanostructured SnO(x) films. *Mateial Researcher Express*, 7, 015027. doi:10.1088/2053-1591/ab6122

Thirumoorthi, M., & Prakash, J. T. J. (2016). Structure, optical and electrical properties of indium tin oxide ultra thin films prepared by jet nebulizer spray pyrolysis technique. *Journal of Asian Ceramic Societies*, 4, 124-132. doi:10.1016/j.jascer.2016.01.001